



ISTITUTO NAZIONALE DI RICERCA METROLOGICA Repository Istituzionale

Use of software-defined radio receivers in two-way satellite time and frequency transfers for UTC computation

This is the author's submitted version of the contribution published as:

Original

Use of software-defined radio receivers in two-way satellite time and frequency transfers for UTC computation / Jiang, Z.; Zhang, V.; Huang, Y. J.; Achkar, J.; Piester, D.; Lin, S. Y.; Wu, W.; Naumov, A.; Yang, S. H.; Nawrocki, J.; Sesia, I.; Schlunegger, C.; Yang, Z.; Fujieda, M.; Czubla, A.; Esteban, H.; Rieck, C.; Whibberley, P.. - In: METROLOGIA. - ISSN 0026-1394. - 55:5(2018), pp. 685-698. [[10.1088/1681-7575/aacbe6](https://doi.org/10.1088/1681-7575/aacbe6)]

Availability:

This version is available at: 11696/59948 since: 2019-02-19T17:40:38Z

Publisher:

IOP

Published

DOI:[10.1088/1681-7575/aacbe6](https://doi.org/10.1088/1681-7575/aacbe6)

Terms of use:

This article is made available under terms and conditions as specified in the corresponding bibliographic description in the repository

Publisher copyright

Institute of Physics Publishing Ltd (IOP)

IOP Publishing Ltd is not responsible for any errors or omissions in this version of the manuscript or any version derived from it. The Version of Record is available online at DOI indicated above

(Article begins on next page)

Use of Software-Defined Radio Receivers in TWSTFT for UTC Computation

Zhiheng JIANG¹, Victor ZHANG^{2*}, Yi-Jiun HUANG³, Joseph ACHKAR⁴, Dirk PIESTER⁵, Shinn-Yan LIN³, Wenjun WU⁶, Andrey NAUMOV⁷, Sung-hoon YANG⁸, Jerzy NAWROCKI⁹, Ilaria SESIA¹⁰, Christian SCHLUNEGGER¹¹, Zhiqiang YANG¹², Miho FUJIEDA¹³, Albin CZUBLA¹⁴, Hector ESTEBAN¹⁵, Carsten RIECK¹⁶, Peter WHIBBERLEY¹⁷

1 BIPM: Bureau International des Poids et Mesures, Sèvres, France, zjiang@bipm.org

2 NIST: National Institute of Standards and Technology, 325 Broadway, Boulder, CO80305, USA, victor.zhang@nist.gov

3 TL: National Standard Time and Frequency Laboratory, Telecommunication Laboratories, Chunghwa Telecom, Chinese Taipei

4 OP: LNE-SYRTE, Observatoire de Paris, Université PSL, CNRS, Sorbonne Université, 61 avenue de l'Observatoire 75014 Paris, France

5 PTB: Physikalisch-Technische Bundesanstalt, Bundesallee 100, 38116 Braunschweig, Germany

6 NTSC: National Time Service Center, Lintong, Xian, China

7 SU/VNIIFTRI: Main Metrological Center for State Service of Time and Frequency, FGUP VNIIFTRI, Russia

8 KRIS Korea Research Institute of Standards and Science

9 AOS: Space Research Center, Astrogeodynamic Observatory, Borowiec, Poland

10 IT/INRIM: Istituto Nazionale di Ricerca Metrologica, 10135 Turin, Italy

11 CH/METAS: Federal Institute of Metrology METAS, Lindenweg 50, 3003 Bern-Wabern, Switzerland

12 NIM: National institute of Metrology, 100029 Beijing, China

13 NICT: National Institute of Information and Communications Technology, Japan

14 PL/GUM: Central Office of Measures, Warsaw, Poland

15 ROA: Real Instituto y Observatorio de la Armada, Spain

16 RISE/SP: Research Institutes of Sweden, Sweden

17 NPL: National Physical Laboratory, United Kingdom

* Corresponding author

ABSTRACT

Two-Way Satellite Time and Frequency Transfer (TWSTFT) is a primary technique for the generation of Coordinated Universal Time (UTC). About 20 timing laboratories around the world continuously operate TWSTFT using Satellite Time and Ranging Equipment (SATRE[†]) modems for remote time and frequency comparisons in this context. The precision of the SATRE TWSTFT as observed today is limited by an apparent daily variation pattern (diurnal) in the TWSTFT results. The observed peak-to-peak variation have been found as high as 2 ns in some cases. Investigations into the origins of the diurnals have so far provided no complete understanding about the cause of the diurnals. One major contributor to the diurnals, however, could be related to properties of the receive part in the modem. In 2014 and 2015, it was demonstrated that bypassing the receive part and the use of Software-Defined Radio (SDR) receivers in TWSTFT ground stations (SDR TWSTFT) instead could considerably reduce the diurnals and also the measurement noise.

In 2016, the International Bureau of Weights and Measures (BIPM) and the Consultative Committee for Time and Frequency (CCTF) Working Group (WG) on TWSTFT launched a pilot study on the application of SDR receivers in the TWSTFT network for UTC computation.

The first results of the pilot study were reported to the CCTF WG on TWSTFT annual meeting in May 2017, demonstrating that SDR TWSTFT shows superior performance compared to that of SATRE TWSTFT for practically all links between participating stations. In particular, for continental TWSTFT links, in which the strongest diurnals appear, the use of SDR TWSTFT results in a significant suppression of the diurnals by a factor of between two and three. For the very long inter-continental links, e.g. the Europe-to-USA links where the diurnals are less pronounced, SDR TWSTFT achieved a smaller but still significant gain of 30 %. These findings are supported by an evaluation of some of the links with an alternate technique based on GPS signals (GPS IPPP) as reported in this paper.

Stimulated by these results, the WG on TWSTFT prepared a recommendation for the 21st CCTF meeting, which proposed the introduction of SDR TWSTFT in UTC generation. With CCTF approval of the recommendation, a roadmap was developed for the implementation of SDR TWSTFT in UTC generation. In accordance with the roadmap, most of the stations that participated in the pilot study have updated the SDR TWSTFT settings to facilitate the use of SDR TWSTFT data in UTC generation. In addition, the BIPM conducted a final evaluation to validate the long-term stability of SDR TWSTFT links, made test runs using the BIPM standard software for the calculation of UTC, now including SDR TWSTFT data, and started to calculate SDR TWSTFT time links as backup from October 2017. The use of SDR TWSTFT in UTC generation will begin in 2018.

Keywords: UTC, TWSTFT, SDR, Diurnal, Uncertainty, Time Transfer

List of acronyms and specific terms:

1 PPS: 1 Pulse Per Second timing signal

A/D: Analog to Digital

BIPM, NIST, TL, OP/LNE-SYRTE, PTB, NTSC, SU/VNIFTRI, KRIS/KRIS, AOS, IT/INRIM, CH/METAS, NIM, NICT, PL/GUM, ROA, RISE/SP, NPL: acronyms of the UTC laboratories, cf. the authorship for their full names.

BPSK: Binary Phase-Shift Keying

CALR: CALibration Result value of station delays for a two-way link, defined in the recommendation ITU-R TF.1153-4

CCTF: Consultative Committee for Time and Frequency

CI: Calibration identifier as defined in the recommendation ITU-R TF.1153-4

DCD: Double Clock Difference, the difference between two time links which are connected to the same clocks at both ends

DCD' : DCD after removing a linear tendency; note that a statistically significant non zero slope indicates weakness of at least one part of equipment involved

Diurnal: A daily variation pattern apparent in the TWSTFT results, dominant uncertainty source in SATRE TWSTFT

ESDVAR: Earth Station Delay VARIation with respect to the earth station delay presented at the time of a calibration, defined in the recommendation ITU-R TF.1153-4

Gain factor or Gain: Ratio of $\sigma(A)/\sigma(B)$ or $\sigma_x(A)/\sigma_x(B)$.

If $\text{Gain} \leq 1$, there is no improvement. Statistically, if $\text{Gain} \geq 1.10$, the improvement is considered as significant.

GPS PPP or PPP for short: GPS carrier-phase Precise Point Positioning solution for time and frequency transfer

GPS IPPP or IPPP for short: GPS carrier-phase Integer Ambiguity PPP solution for time and frequency transfer

GPU: Graphic Processing Unit

IF: intermediate frequency at 70 MHz for TWSTFT

ITU-R TF: International Telecommunication Union Radiocommunication Sector, Time signals and frequency standards emissions Series

Ku-band: frequency band (10.7 – 14.5 GHz) used for space radiocommunications

MJD: Modified Julian Date

PRN: PseudoRandom Noise

REFDELAY: Delay of the modem time reference with respect to UTC(k), defined in the recommendation ITU-R TF.1153-4

SATRE: SATellite Time and Ranging Equipment, brand name of a modem developed by Time Tech GmbH, Stuttgart, Germany

SATRE TWSTFT, SATRE link or SATRE for short: TWSTFT using the SATellite Time and Ranging Equipment (modems)

SDR TWSTFT, SDR link or SDR for short: TWSTFT with data from Software-Defined Radio receivers

Slope affecting factor: $\sigma(\text{DCD}') / \sigma(\text{DCD})$.

TWSTFT or TW for short: Two-Way Satellite Time and Frequency Transfer

UTC: Coordinated Universal Time

WG on TWSTFT: CCTF Working Group on TWSTFT

$\sigma(A)$: Standard deviation of a time series A

$\sigma_x(A)$ or TDev(A): Time deviation of a time series A (see e.g. requirement ITU-R TF.538, or NIST Special Publication 1065 (2008): Handbook of frequency stability analysis)

1. Introduction

TWSTFT is a primary technique for the realization of UTC [1, 2, 6]. Since 2003 TWSTFT data provided by the international timing community have been used in this context. TWSTFT is done by transmission of pseudorandom noise (PRN) signals modulated via binary phase-shift keying (BPSK) onto the carrier signal in Ku-band. The phase modulation is synchronized with the local clock's 1 PPS output. Each station uses a dedicated PRN code for its BPSK sequence in the transmitted signal. In the receive part of the modem, the BPSK sequence of the remote station is generated and correlated with the received signal. As a result, the time-of-arrival of the received signal is obtained with respect to the local clock. All TWSTFT stations involved in the current study have been equipped with SATRE modems. Diurnal variations in TWSTFT results have been observed in many links with varying amplitudes and several causes could potentially contribute to their existence. They are the dominant source of time transfer uncertainty, with peak-to-peak amplitudes of up to 2 ns in the case of the widely used BPSK modulations of 1 MChip/s.

An SDR receiver can operate in parallel with a SATRE modem, and data generated that way are free from the effects of processing in the SATRE receive part. In each station the transmission signal is generated by the SATRE modem and the down-converted received signal is split and fed to both the SDR setup and SATRE modem. The key components of the SDR consist of an analog to digital (A/D) sampler recording the received PRN signal at the 70 MHz intermediate frequency (IF), and a graphic processing unit (GPU) card installed in a computer for processing the TWSTFT measurements with dedicated software developed by TL [3, 4]. In addition, one or two amplifiers and a bandpass filter are used to optimize the input signal to the A/D sampler. The arrival time of the signal is thus determined by SATRE modem and SDR receiver independently [3, 4], as illustrated

[†]Disclaimer: Commercial products are identified for the sake of technical clarity. No endorsement by the authors or their institutes are implied. We further caution the readers that none of the described equipment's apparent strengths or weaknesses may be characteristic of items currently marketed.

in Figure 1.1. With the application of SDR receivers in TWSTFT, a significant reduction of the diurnals and the measurement noise in Asian TWSTFT links was observed. Based on the encouraging results and a first validation of the method by the BIPM, the BIPM and the CCTF WG on TWSTFT launched a pilot study in February 2016. Its goal was to investigate the improvements to be gained from using SDR TWSTFT in Asia-to-Asia, Asia-to-Europe, Europe-to-Europe and Europe-to-USA links with different satellites, linking a number of laboratories as illustrated in Figure 1.2.

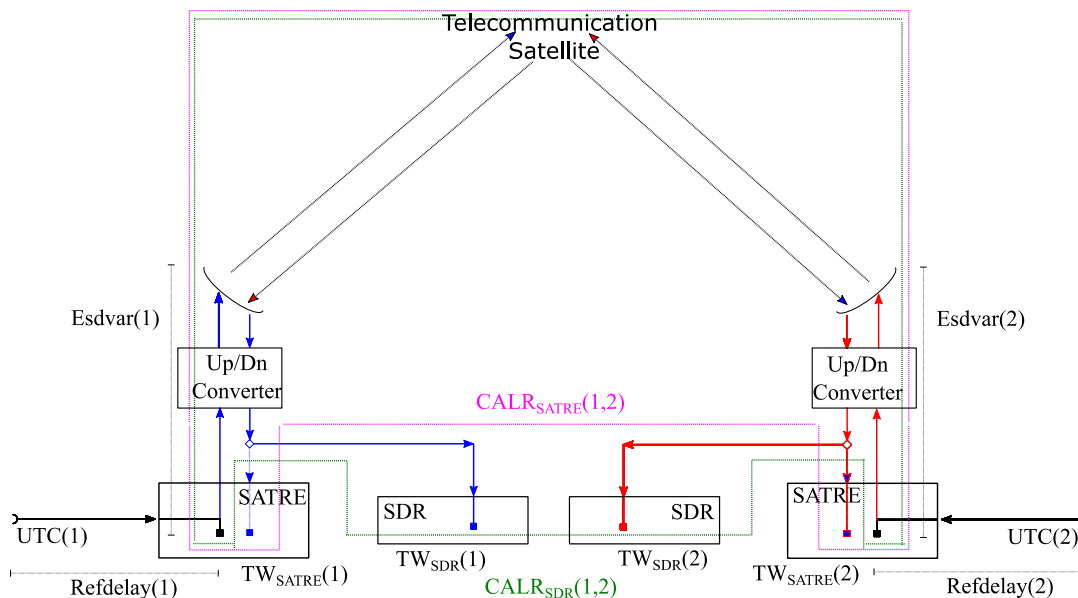


Figure 1.1 Illustration of the main signal paths of a TWSTFT link based on the combination of SATRE modems with SDR receivers for comparison of two separated time scales UTC(1) and UTC(2)

The following 16 timing laboratories have installed SDR receivers and have participated in routine SDR TWSTFT measurements: TL, NICT, KRISS (KRIS), NTSC and NIM in Asia; PTB, OP, VNIIFTRI (SU), INRIM (IT), METAS (CH), AOS, PL (GUM), RISE (SP), ROA and NPL in Europe; and NIST in the USA. The characters in brackets represent the designation of their time scales (e.g. UTC(SU)). In the pilot study, Ku-band transponders on three satellites were used. The Asia-to-Asia links used 2.5 MHz bandwidth on the Eutelsat 172A (E172A) satellite[†] until November 2017. The E172A was then replaced by the Eutelsat 172B (E172B) satellite[†]. The Asia-to-Europe links used 2.5 MHz bandwidth on the Express AM22 satellite[†] until June 2017, and spectrally filtered signals with a 2.5 MChip/s BPSK were transmitted. The Europe-to-Europe and the Europe-to-USA links use 1.7 MHz and 1.6 MHz bandwidths, respectively, on the Telstar 11N (T-11N) satellite[†], and thus a smaller modulation rate of only 1 MChip/s can be used. The Europe-to-USA links are through two different transponders whereas one transponder handles the Europe-to-Europe links. The successor to the AM22 satellite has been selected as the ABS-2A satellite[†] and some of the Asia-to-Europe TWSTFT links have been reinstalled in March 2018, but no data are available at the time of the writing.

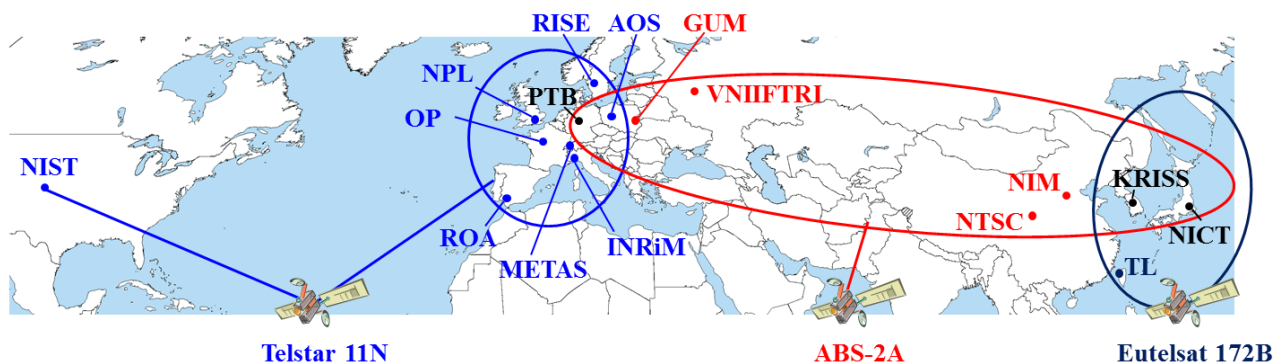


Figure 1.2 Participating stations in the SDR pilot study (status of March 2018). The links/circle in blue are for the Europe-to-Europe and Europe-to-USA SDR TWSTFT. The laboratories circled in red are for the Asia-to-Europe SDR TWSTFT. Until June 2017, the AM22 satellite was used in place of the ABS-2A satellite. The laboratories in the black circle are for the Asia-to-Asia SDR TWSTFT. In November 2017, the E172B satellite replaced the E172A satellite.

Continental (within Asia and Europe) and also transcontinental (Asia-to-Europe, Europe-to-USA) SDR time links have been established. Thus, this pilot study has a global coverage involving laboratories from countries around the world. SDR TWSTFT

proved to provide superior or at least similar performance compared to the that of SATRE TWSTFT for all links [7, 8]. In the case of the continental links, such as those within Europe where the strongest diurnals are present, the magnitude of the diurnals in SDR TWSTFT was reduced by a factor of two to three. For the very long inter-continental links, such as the transatlantic links where the diurnals' impact is less, SDR TWSTFT displays a smaller gain of only 30 %, but it is still significant.

Based on these findings, the CCTF WG on TWSTFT prepared a recommendation "On improving the uncertainty of Two-Way Satellite Time and Frequency Transfer (TWSTFT) for UTC generation" [5] for the 21st CCTF meeting held on 9-10 June 2017 at the BIPM, where the recommendation was approved. Thereafter, the process of implementing SDR TWSTFT into UTC generation was started. Setup changes are necessary to install SDR receivers into operational TWSTFT ground stations. Furthermore, the data computation, e.g. for calibrated time transfer, requires caution during data processing based on standard procedures, which is not trivial. An *ad hoc* group was therefore established in May 2017 to develop a roadmap for the coordinated operation and schedule needed to implement the use of SDR TWSTFT in UTC. Its attention was focused on the practical issues including verification of the SDR hardware setup, the software performance in the participating laboratories, a standard data format and submission procedure, the software package for *Circular T* computation at the BIPM, and the attainable uncertainty based on a final evaluation using the most recent continuous data collected over six months.

In this paper, we report the state-of-the-art of the SDR TWSTFT method and the main results of the final evaluation. We compare SDR TWSTFT with the recently introduced integer ambiguity solution for GPS precise point positioning, IPPP [12], which is considered as an alternative high-accuracy method for frequency and time comparisons, and represents a further development of the 'conventional' PPP. The use of IPPP solutions is preferred for comparisons with GPS links. In fact, the phase ambiguities of GPS carrier signals are physically integer number of cycles, which are taken into account in the IPPP technique, while the standard PPP solves the ambiguities as real values. The associated error in PPP solutions may be summed up as a random walk instability for reasonable averaging times. The IPPP method may eliminate this bias. It is generally accepted that IPPP is diurnal free and the most precise of the presently available GPS comparison techniques. IPPP data are, however, not yet produced on a regular basis. We use IPPP when possible in the discussions below, and only use PPP solutions when it is not available.

We first discuss the key issues of the pilot study, such as the methods used in the BIPM evaluations, calibration of SDR TWSTFT links, and the attainable uncertainty, in Section 2 of this paper. Section 3 provides the evaluation results based on the monthly SDR TWSTFT data sets. The evaluation results of SDR TWSTFT long-term stability are presented in Section 4. Finally, we summarize the study of the use of SDR TWSTFT in UTC generation in Section 5.

2. Key issues in the SDR pilot study

2.1 Methods of validation and evaluation

The validation and evaluation of SDR TWSTFT are based on analysing the differences of time links operated in parallel between two clocks. In this way, the properties of the clocks do not matter. The analysis of so-called double clock differences (DCD) have been made over selected baselines between (a) the SATRE and the SDR links, and (b) the SATRE and/or SDR TWSTFT against GPS PPP and/or GPS IPPP time transfer links. Examples of time links used in the calculation of UTC are also presented.

The validation and evaluation employs the following statistical measurands:

- The σ_x of time links, the $\sigma(\text{DCD})$ and the $\sigma_x(\text{DCD})$;
- The following four indicators of the assessment of the quality and the level of the improvement :
 1. σ_x for evaluation of the time link instabilities at different averaging times (τ)
 2. $\sigma(\text{DCD})$ and $\sigma(\text{DCD}')$ for revealing the agreement of SDR TWSTFT with SATRE TWSTFT, GPS PPP, and GPS IPPP
 3. Deviation from zero and σ of triangle closures for indication of systematic offsets and noise level of the links
 4. σ of discrepancies between SATRE TWSTFT, SDR TWSTFT and GPS PPP for the long-term stability
- Gain factors: the ratios of $\sigma(\text{SATRE})/\sigma(\text{SDR})$, $\sigma_x(\text{SATRE})/\sigma_x(\text{SDR})$

The majority of the data used are monthly and long-term data sets. The monthly data is the basis of the BIPM *Circular T* computation whereas the latter is employed for a long-term stability analysis. Long-term stability of time transfer techniques is a very important characteristic for their application in the production of UTC. The data were collected mainly in 2016 and 2017. In particular, the latest data sets investigated in this work are from the 6-month period between July and December 2017.

2.2 Setup of SDR TWSTFT and data Processing

The SDR receivers had been installed in 16 TWSTFT laboratories by the end of October 2017. Most of them have gathered more than one year of data. Unfortunately, the Asia-to-Europe links are currently interrupted due to a change of satellite.

The SATRE TWSTFT data are reported in the format defined in the Recommendation ITU-R TF.1153-4 [6] (ITU for short).

Following the roadmap, it was decided to adopt the same file name and format for reporting the SDR TWSTFT data in UTC computation as those already in use for SATRE measurements. A comment line in the file header and the SDR identifier are used to indicate the SDR measurements. The parameters of CALR, ESDVAR, REFDELAY etc. are suitably adapted. For the SDR TWSTFT data, the session length of a single measurement recording is 300 s. The measurement process is carried out automatically by the SDR software obs2ITU, release V2018.1, developed and distributed by TL to all participants. It records measurements and the corresponding parameters and identifiers in the data file. The BIPM UTC computation software, Tsoft, can recognise the SATRE and SDR TWSTFT data and perform the time transfer computation and all other operations required to publish the results on the BIPM website with the standard procedure. More details can be found in [8].

2.3 Calibration of SDR TWSTFT links

The use of SDR TWSTFT links in UTC generation requires that the signal delays in the ground stations have been determined. According to the TWSTFT calibration guidelines [2], a SDR link calibration can be made using a ‘2-step procedure’:

1. For UTC links:
 - a) if the SATRE link is calibrated, the SDR link should be aligned to it by using the same CALR and to determine the corresponding ESDVAR value. In this case, the calibration identifier (CI) of the SDR link is the same as that of the SATRE link;
 - b) if the SATRE link is not calibrated, both of the SATRE and the SDR links should be calibrated together by using a TWSTFT mobile station or a GPS calibrator with the ‘link’ method;
2. The non-UTC link delay should be calibrated by the triangle closure calibration (TCC) method;

In the final evaluation and also in the UTC backup computation, the SDR links are calibrated with respect to the related SATRE links using the data set from September 2017. Table 2.2 lists the SDR calibration corrections for the UTC links in Europe and the TL-KRIS link in Asia that were calibrated using the PPP link. For example, the calibrated AOS-PTB SDR TWSTFT link results are achieved by subtracting 54.449 ns from the raw SDR solutions. The column “*N*-Point” contains the number of points used in the calibration computations. Here, and in the following discussion, *yymm* stands for year and month.

Table 2.2 The SDR link calibration corrections

Link	Correction /ns	<i>N</i> -Point	σ /ns	CI of SATRE link	Data set used / <i>yymm</i>
AOS-PTB	-54.449	329	0.659	449	1709
CH-PTB	-128.909	356	0.454	284	1709
IT-PTB	-188.926	376	0.519	434	1709
NIST-PTB	-113.862	245	0.108	393	1709
OP-PTB	2263.247	305	0.428	437	1709
TL-KRIS	-2441.649	4101	0.241	GPS PPP	1710

2.4 Uncertainty

We define the *conventional* uncertainties u_A and u_B , which are values assigned and used in BIPM *Circular T* and which are usually substantially higher than the estimated uncertainties in order to allow the use of a general value for all links of the same kind.

For the UTC SATRE links, the *conventional* value of u_A is 0.5 ns, and u_B is 1.0 ns (when using a TWSTFT mobile station for calibration) or 1.5 ns (with a GPS calibrator). These values are assigned to the time scale differences UTC-UTC(k). They are derived from a detailed report on the link data and reported in Section 5 of BIPM *Circular T* [1].

We assign the corresponding values of $u_A = 0.2$ ns and $u_B = 1.0$ ns or 1.5 ns, respectively, for SDR links. In fact, as reported in [7, 8] and concluded in this paper, for short baselines, such as OP-PTB, a gain factor of two or three is obtained in the stabilities of SDR TWSTFT compared with SATRE TWSTFT. For long baselines, such as NIST-PTB which has a much smaller diurnal than most of the other links (e.g. OP-PTB), the stability of the SATRE link is already below 0.2 ns; see [8] and the discussion in the section below. We consider that for u_B , the same conventional value is valid for both the SATRE and the SDR links because, as mentioned above, the conventional u_B of the SATRE link is always higher than the estimated one, and an additional uncertainty component for transferring a calibration to the SDR equipment will not increase the uncertainty significantly. The conventional value of u_B for the SDR TCC calibration is 2.0 ns, the same as when using SATRE data [1, 2]. The u_B of SDR links may be improved if a direct SDR link calibration using a mobile station equipped with the SDR receiver is performed. This study is ongoing.

3. TWSTFT monthly data analysis and comparisons

UTC is computed and published monthly. The monthly data set is therefore taken as the base for this analysis of the SDR TWSTFT evaluation. We use the SATRE TWSTFT, SDR TWSTFT, GPS PPP, and IPPP data types and the validation methods given in Section 2.1. We will discuss the gain factors of SDR TWSTFT versus the SATRE TWSTFT through the following numerical examples. All time scales involved in the study, and in particular those referred to in the examples are realized based on signals from active hydrogen masers, with different strategies for steering towards UTC.

3.1 Comparison between SATRE and SDR time links

Figure 3.1.1 plots both the SATRE and the SDR links for the clock comparison of [UTC(OP)-UTC(PTB)] during a 100-day period between MJDs 57630 and 57730 (UTC data sets: 1609-1611) with 1151 TWSTFT results in total. The OP-PTB SATRE TWSTFT is a Europe-to-Europe UTC link. We observe on the upper part of the figure that the SATRE TWSTFT is very noisy. However, the enlarged plot shows that the scatter is not white noise but dominated by diurnals of 2 ns peak-to-peak. In the SDR link the diurnal variations are no longer evident and the peak-to-peak variation become less than 0.4 ns. This is confirmed by the TDev plot shown in Figure 3.1.1.

By virtue of the technique involved, SDR TWSTFT can bring an improvement in TDev only up to averaging times of the order of one day. After that, the properties of the time scales involved contribute significantly to the TDev value. We see in Figure 3.1.1 that at an averaging time of > 64 hours the two curves start to coincide. Table 3.1.1 gives the gain in TDev at different averaging times from two hours to 32 hours. The TDev at two hours' averaging time is 307 ps for SATRE TWSTFT and 94 ps for SDR TWSTFT, representing an improvement in the short-term stability by a gain factor of 3.3. The maximum and minimum gains are 5.2 and 2.1 for eight and 32 hours, respectively. The mean gain for different averaging times is 3.7.

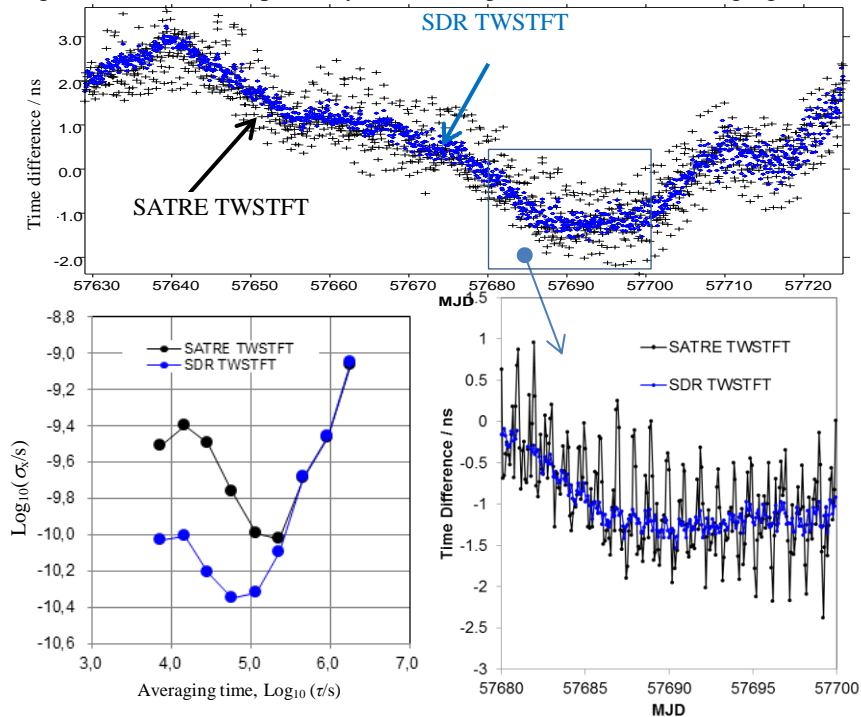


Figure 3.1.1 The SDR and the SATRE links and the corresponding TDev over the baseline of OP-PTB via satellite T-11N

Table 3.1.1 Gain factor in TDev at different averaging times for the OP-PTB SDR versus SATRE links

Average time (1)	$\sigma_x(\text{SATRE})$ /ps (2)	$\sigma_x(\text{SDR})$ /ps (3)	Gain = (2)/(3)
2 h	307	94	3.3
4 h	398	99	4.0
8 h	322	62	5.2
16 h	171	44	3.9
32 h	100	48	2.1
Mean			3.7

The AOS-PTB SATRE TWSTFT is also a Europe-to-Europe UTC link. In Figure 3.1.2, we compare the AOS-PTB SATRE and the SDR TWSTFT links between MJDs 57785 and 57815 (UTC data set 1702). The diurnal in the SATRE link is clearly shown by the two ns or even larger peak-to-peak variations. As seen in the figure, the diurnals have almost disappeared in the SDR TWSTFT difference. There are some disturbances in the SDR results in the first half of the data set between MJDs 57785 and

57800; the cause is unknown. As shown in Table 3.1.2, the mean gain factor in TDev is 2.9.

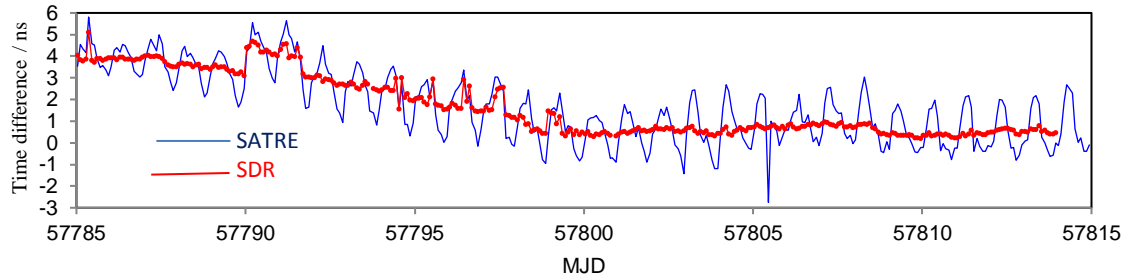


Figure 3.1.2 The SATRE and the SDR links over the baseline of AOS-PTB via satellite T-11N

Table 3.1.2 Gain factor in TDev at different averaging times for the AOS-PTB SDR versus SATRE links

Average time (1)	$\sigma_x(\text{SATRE})$ /ps (2)	$\sigma_x(\text{SDR})$ /ps (3)	Gain =(2)/(3)
2 h	422.6	181.6	2.3
4 h	537.2	147.3	3.7
8 h	955.2	165.0	5.8
16 h	523.8	153.2	3.4
32 h	376.3	207.5	1.8
Mean			2.9

The SU-NIM SATRE TWSTFT link is a long-distance Europe-to-Asia link between SU in Russia and NIM in China via the satellite AM22. Figure 3.1.3 shows a comparison of the SDR and SATRE TWSTFT (for an 8-day segment of UTC data set 1702). The gain of SDR TWSTFT over SATRE TWSTFT is clearly significant for the SU-NIM baseline. As shown in Table 3.1.3, gain factors have been calculated for the available averaging times up to 16 hours although there are indications that the two time scales involved are less stable than those in the previous examples. A mean gain factor in TDev of 2.0 is computed.

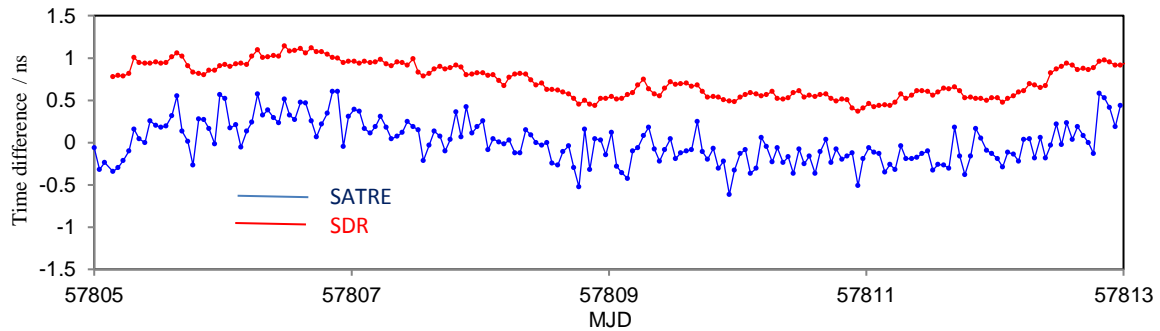


Figure 3.1.3 The SATRE and the SDR links over the baseline of SU-NIM via satellite AM22

Table 3.1.3 Gain factor in TDev at different averaging times for the SU-NIM SDR versus SATRE links

Average time (1)	$\sigma_x(\text{SATRE})$ /ps (2)	$\sigma_x(\text{SDR})$ /ps (3)	Gain =(2)/(3)
1 h	111.1	26.4	4.2
2 h	92.0	32.2	2.9
4 h	59.4	34.2	1.7
8 h	50.2	47.0	1.1
16 h	47.8	48.5	1.0
Mean			2.0

3.2 Comparison between SATRE/SDR links and the PPP/IPPP links

Unlike the examples in Section 3.1 where the TWSTFT links are compared, we now use the GPS IPPP or PPP as reference in DCD calculations to compare SATRE and SDR links over the baselines of TL-NICT in Asia, OP-PTB in Europe, and NIST-PTB across the Atlantic.

Being independent from TWSTFT, the GPS PPP or IPPP solutions are able to validate the improvement of SDR TWSTFT. The GPS solutions' statistical uncertainty is small ($u_A \leq 0.3$ ns [1]) and it is almost unaffected by diurnal variations. When we make a choice between SATRE and SDR links using a GPS solution as the reference, the TWSTFT link whose statistical uncertainty is closer to that of the GPS is considered the better one. Comparing TWSTFT to GPS also allows for the investigation of the short-term and long-term instabilities of SDR TWSTFT in view of the time link calibration, a key issue in the UTC time transfer. We emphasize that SATRE/SDR TWSTFT and GPS PPP/IPPP are independent, but PPP/IPPP are not errorless. Therefore, attributing the standard deviation of the DCD to only from the TW measurements gives a more conservative estimation.

Table 3.2.1 Gain factor in TDev for the DCD of SATRE versus SDR links against the PPP link over the baseline of TL-NICT

Averaging time (1)	$\sigma_x(\text{SATRE-PPP})$ /ps (2)	$\sigma_x(\text{SDR-PPP})$ /ps (3)	Gain = (2)/(3)
1 h	140	40	3.5
2 h	90	45	2.0
6 h	125	38	3.3
12 h	79	48	1.6
24 h	68	59	1.2
Mean			2.3

Table 3.2.1 gives the gain factor in TDev for the DCD of SATRE versus SDR links against the PPP link over the baseline of TL-NICT in February 2016 (UTC data set: 1602). The intra-Asia links via the satellite E172A are characterized by their much lower short-term instability and much smaller number of users compared to the intra-Europe links via satellite T-11N. As noted previously, in Asia the TWSTFT links are operated with codes modulated at 2.5 MChip/s, which leads to a reduced measurement noise compared with 1 MChip/s operation prevailing in the European and Europe-to-USA links [14]. This is true for both the SATRE and the SDR links. From the table, the highest gain occurs at the averaging time of one hour and the lowest at one day. In fact, the diurnal is no longer an issue beyond one day. The mean value of the gains is 2.3.

Almost one month of IPPP solutions are available in December 2017 over the UTC baselines of OP-PTB and NIST-PTB. By analysing the DCD between the SATRE, SDR and IPPP links, we can evaluate the gain factors of SDR TWSTFT versus SATRE TWSTFT.

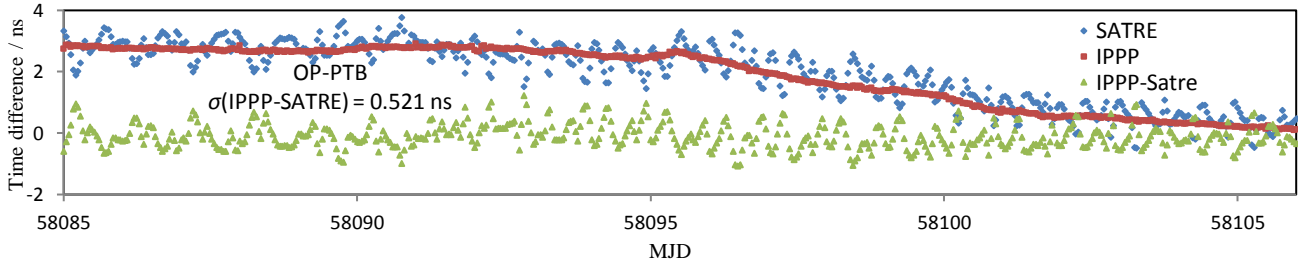


Figure 3.2.1 SATRE and IPPP links and the DCD over the baseline of OP-PTB with $\sigma(\text{DCD}) = 0.521$ ns.

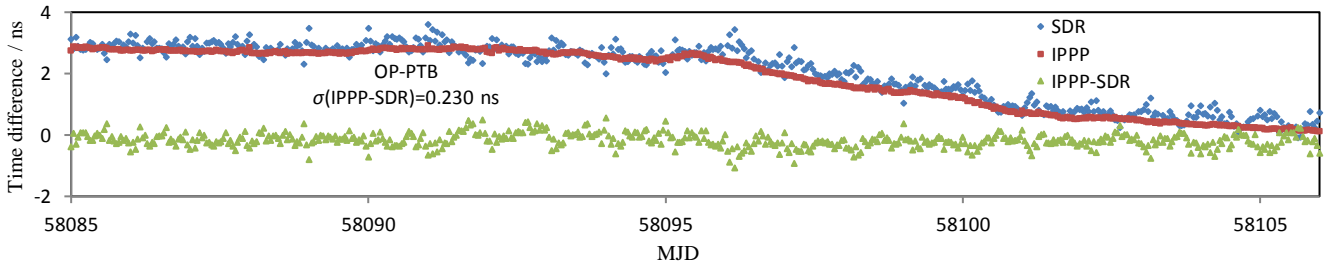


Figure 3.2.2 SDR and IPPP links and the DCD over the baseline of OP-PTB with $\sigma(\text{DCD}) = 0.230$ ns

For the baseline of OP-PTB, Figures 3.2.1 and 3.2.2 show the comparisons of SATRE, SDR and IPPP links as well as the DCD(IPPP-SATRE) and DCD(IPPP-SDR); the $\sigma(\text{IPPP-SATRE}) = 0.521$ ns and $\sigma(\text{IPPP-SDR}) = 0.230$ ns, respectively. The gain factor is 2.3.

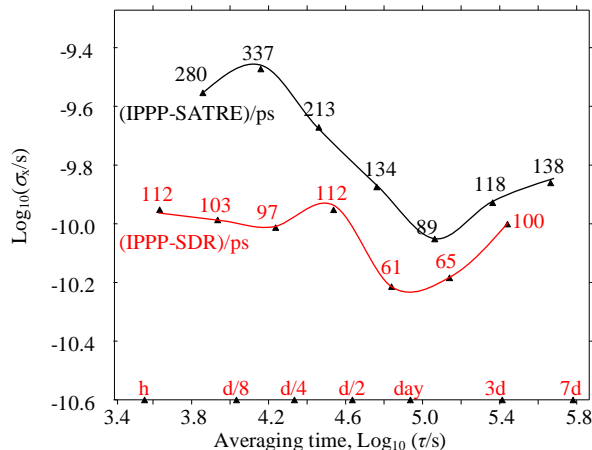


Figure 3.2.3 TDev of the DCDs data plotted in Figures 3.2.1 and 3.2.2.

The axes of the plot are expressed in logarithmic scale. The numbers in the plot represent σ_x values in picoseconds.

Figure 3.2.3 shows the TDev values corresponding to the DCDs in Figures 3.2.1 and 3.2.2. Table 3.2.2 gives the gain factor at different averaging times from two hours to 32 hours. The maximum gain is 3.5 at four hours and the mean gain of the TDev is 2.4. As the TDev values for the IPPP-SDR data were computed for different averaging times than for the IPPP-SATRE data, the TDev values of IPPP-SDR were interpolated to get the numbers which are listed in Table 3.2.2.

Table 3.2.2 Gain factor in TDev for the DCD of SATRE and SDR links against the IPPP link over the baseline of OP-PTB corresponding to Figure 3.2.3

Averaging time (1)	$\sigma_x(\text{IPPP-SATRE})$ /ps (2)	$\sigma_x(\text{IPPP-SDR})$ /ps (3)	Gain = (2)/(3)
2 h	280	104	2.7
4 h	337	96	3.5
8 h	213	112	1.9
16 h	134	62	2.2
32 h	89	62	1.4
Mean			2.4

Tables 3.2.1 and 3.2.2 contain the gain factors in TDev of the DCDs. Noting that the mean values of gain are around 2.3, although the data used in the analyses were from two different periods, February 2016 and December 2017, over the two continental baselines.

Figure 3.2.4 shows the DCD of the SATRE and SDR links against the IPPP link over the transatlantic baseline of NIST-PTB with $\sigma(\text{IPPP-SATRE}) = 0.355$ ns and $\sigma(\text{IPPP-SDR}) = 0.267$ ns. The gain factor is then $0.355 \text{ ns}/0.267 \text{ ns} = 1.3$, an improvement of 30 % obtained when referring to IPPP. The improvement is calculated by the gain factor minus one. Figure 3.2.5 is the corresponding TDev plot. In general, the stabilities given by the TDev for SDR TWSTFT are somewhat improved with respect to the SATRE TWSTFT at all averaging times, and the peak-to-peak diurnal variation is reduced by about 30 % in SDR TWSTFT when compared to SATRE TWSTFT.

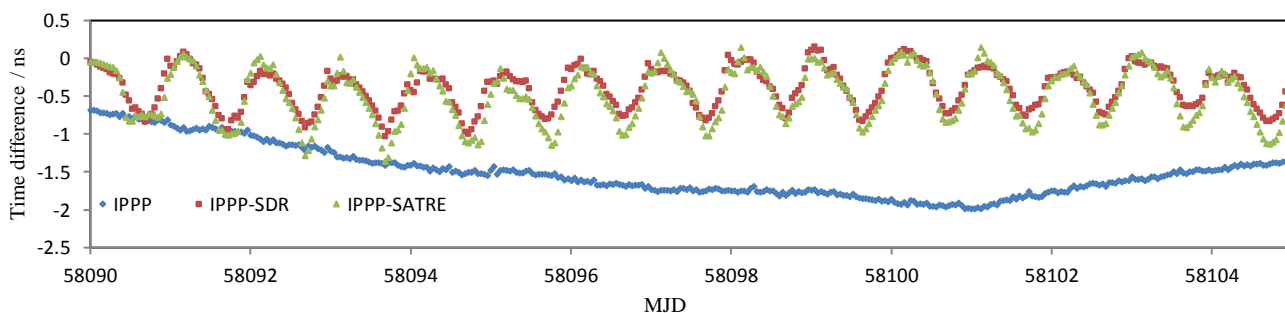


Figure 3.2.4 DCDs of SATRE and SDR links against IPPP link over the baseline of NIST-PTB with $\sigma(\text{IPPP-SATRE}) = 0.355$ ns and $\sigma(\text{IPPP-SDR}) = 0.267$ ns

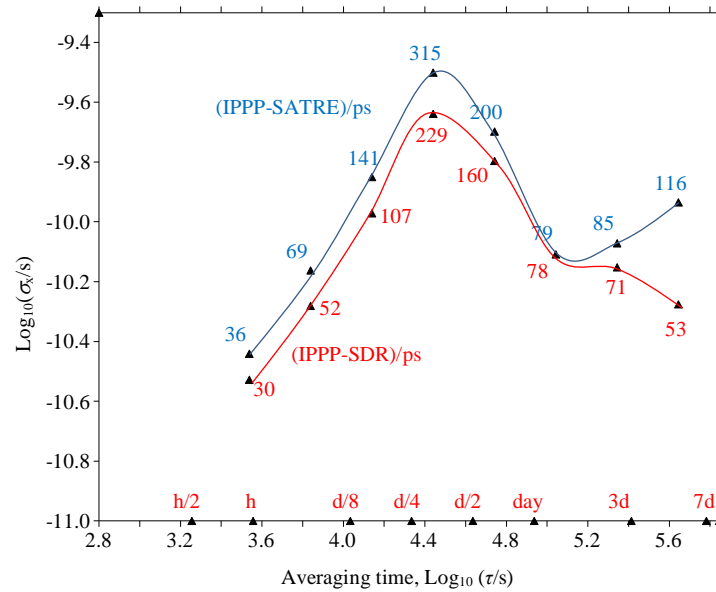


Figure 3.2.5 TDev of the DCDs in Figure 3.2.4 over the baseline of NIST-PTB.

Figures 3.2.4 and 3.2.5 show using different parameters (TDev and standard deviation) that the SDR TWSTFT reduces the maximum amplitude of the diurnal by a factor of 1.3 on average, although the residual diurnal in the SDR link is still strong and dominant in the transatlantic TWSTFT links. However, the gain is clear and statistically evident.

Table 3.2.3 Gain factors of TDev in Figure 3.2.5

Averaging time (1)	$\sigma_x(\text{IPPP-SATRE})$ /ps (2)	$\sigma_x(\text{IPPP-SDR})$ /ps (3)	Gain = (2)/(3)
1 h	36	30	1.2
2 h	69	52	1.3
4 h	141	107	1.3
8 h	315	229	1.4
16 h	200	160	1.3
32 h	79	78	1.0
Mean			1.3

Table 3.2.3 lists the gain factors of TDev in Figure 3.2.5. The mean gain in TDev is 1.3 while the gain computed by the σ is 1.3, thus, on average an improvement of about 30 % is obtained. This is statically significant.

Both the intra-Europe TWSTFT links and the Europe-to-USA TWSTFT links use the same satellite T-11N. However, the diurnals affect the latter much less. Taking examples of the OP-PTB and NIST-PTB SATRE links, the diurnal peak-to-peak amplitude was occasionally up to two ns in the first while only about 0.7 ns in the second. Without knowing clearly the mechanisms inside the SATRE receive electronics, a possible explanation for this finding lies in the fact that at any given time only two links are operated simultaneously across the Atlantic (to NIST and the United States Naval Observatory) whereas 4 to 6 intra-European links can be active at a given time. The simultaneous reception of 8 to 12 modulated signals, even with *a priori* orthogonal PRN codes, might challenge the correlation electronics of the SATRE modem. Regarding remaining diurnals along Europe-to-USA links one should recall that the signals East-West and West-East are routed through two different transponders on the satellite whereas one transponder handles the Europe-to-Europe TWSTFT.

3.3 Comparison of the triangle closures given by the SATRE and SDR measurements

A triangle closure is the sum of the three links that compose a triangle. In theory, a triangle closure, that is, $[A - B] + [B - C] + [C - A]$, should be zero (see e.g. [15]). Unlike a GPS triangle configuration, the three links in a TWSTFT triangle are at least partly independent and a non-zero closure indicates there are systematic and statistical errors, where the statistical error contains, and is in fact dominated by, the diurnals. Therefore, the closure is another excellent indicator of the advantages of using SDR TWSTFT.

Table 3.3.1 gives the statistical results of three triangles covering three regions of Asia, Europe and USA, through three different satellites, cf. Figure 1.2. Data between MJDs 57645-57733 are used in the triangle analysis. The standard deviation of the closures using the T-11N satellite is 2.5 times higher than that obtained using the AM22 and E172A satellites. This agrees with the observations discussed in Section 3.2 that the Asian links are more stable than the European links. It is interesting to note that although the three triangles are in quite different configurations, the gain factors are quite similar, in a range between 4.3 and 4.8, with a mean of 4.5. We conclude that the chiprate of the PRN codes and bandwidth of the TWSTFT signals used define the

general level of measurement precision, and the difference in the measurement technique (SATRE and SDR) determines the achievable gain.

Table 3.3.1 Gain factor of the SDR vs. the SATRE links given by the triangle analysis

Triangles/Satellites (1)	$\sigma(\text{SATRE})$ /ps (2)	$\sigma(\text{SDR})$ /ps (3)	Gain factor = (2)/(3)
OP-NIST-PTB /T-11N	470	110	4.3
NICT-KRIS-TL /E172A	190	40	4.8
PTB-NTSC-SU /AM22	180	40	4.5
Mean			4.5

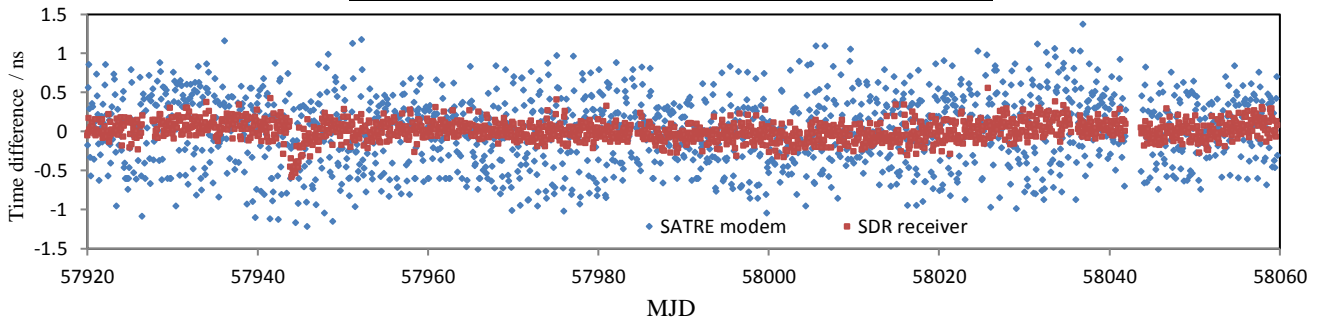


Figure 3.3 Comparison of the OP-NIST-PTB triangle closure formed by SATRE links (blue) and SDR links (red) over a period of 4.5 months from June to November 2017

Figure 3.3 shows a comparison of the SATRE TWSTFT and SDR TWSTFT triangle closures for the OP-NIST-PTB triangle in a period of four and half months between MJDs 57920 and 58060 (June and November 2017). It should be noted that in May 2017, the PTB01 station was replaced by the PTB05 station. The calibration correction values calculated by the BIPM were implemented on MJD 57997. A time step of 0.61 ns has been corrected in all SATRE links with PTB. With $\sigma(\text{SATRE}) = 0.566$ ns and $\sigma(\text{SDR}) = 0.156$ ns, the gain factor is $0.566 \text{ ns}/0.156 \text{ ns} = 3.6$ for the triangle closure.

Table 3.3.2 Summary of the gain factor of SDR versus the SATRE links based on the monthly data analysis

Gain factor computation method	Link used in the analysis	Mean Gain factor
$\sigma_x(\text{SDR})/\sigma_x(\text{SATRE})$	OP-PTB, AOS-PTB and SU-NIM	3.7, 2.9, 2.0
$\sigma_x[\text{DCD}(\text{SDR-PPP}/\text{IPPP})]/\sigma_x[\text{DCD}(\text{SATRE-PPP}/\text{IPPP})]$	TL-NICT, OP-PTB	2.3, 2.4
$\sigma_x[\text{DCD}(\text{SDR-PPP}/\text{IPPP})]/\sigma_x[\text{DCD}(\text{SATRE-PPP}/\text{IPPP})]$	NIST-PTB	1.4
$\sigma[\text{DCD}(\text{SDR-IPPP})]/\sigma[\text{DCD}(\text{SATRE-IPPP})]$	OP-PTB	2.3
$\sigma[\text{DCD}(\text{SDR-IPPP})]/\sigma[\text{DCD}(\text{SATRE-IPPP})]$	NIST-PTB	1.3
$\sigma(\text{SDR triangle closure})/\sigma(\text{SATRE triangle closure})$	OP-NIST-PTB, NICT-KRIS-TL, PTB-NTSC-SU	4.5
Mean		2.5

In this section, we studied the direct comparison between SDR TWSTFT and SATRE TWSTFT links, the comparison of DCDs with GPS PPP or IPPP as reference, as well as the comparison of the triangle closure of SDR and SATRE links using the monthly data sets. We confirmed again that the SDR TWSTFT improves the stability of SATRE TWSTFT in the short-term (over averaging times up to about three days) by reducing the diurnals and the measurement noise. The improvements from these analyses are summarized in Table 3.3.2. The mean value of the gain factors obtained from different evaluations is 2.5.

4. Long-term stability of the SDR TWSTFT links

The long-term stability of SDR links is no doubt one of the most important issues in UTC time transfer. Once a SDR link has been calibrated, it should remain stable. By using the following numerical examples, we investigate the consistency of SDR TWSTFT with respect to SATRE TWSTFT and GPS PPP links. It has been reported that there are long-term variations between TWSTFT and GPS links. Studies [9, 10] have demonstrated that a slope (a linear deviation as a function of time) of up to two ns per year is possible. This slope should be taken into account when studying the long-term DCD between TWSTFT and GPS PPP links. In the following examples, we use the 6-month dataset obtained during July-December 2017 to study the long-term stability of SDR links. The SDR links are calibrated according to the discussions in Section 2.2.

4.1 Long-term consistency between SDR and SATRE TWSTFT links

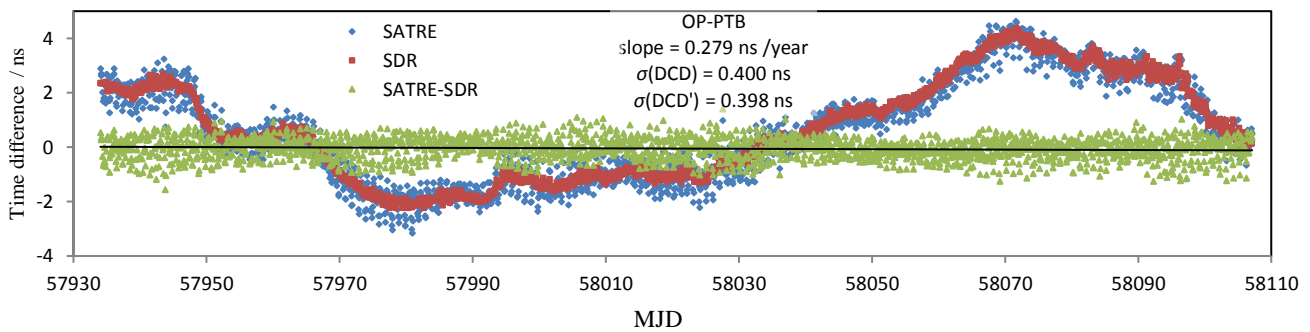


Figure 4.1.1 Six-month SATRE and SDR results and the DCD(SATRE-SDR) over the baseline of OP-PTB

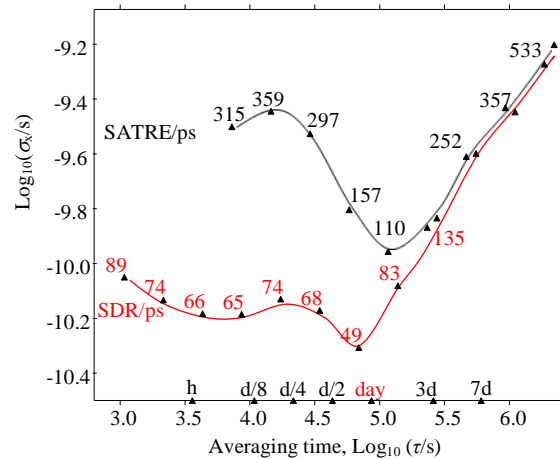


Figure 4.1.2 TDev of the SDR and SATRE TWSTFT results in Figure 4.1.1.

Figure 4.1.1 shows the 6-month SATRE and SDR TWSTFT results and the DCD over the baseline of OP-PTB. Here the DCD is the direct difference between SATRE and SDR links. A linear regression is made over the DCD to determine a possible slope between the two links. A slope of 0.279 ns per year is found. The DCD' is the DCD after removing the slope. The $\sigma(\text{DCD}) = 0.400$ ns and the $\sigma(\text{DCD}') = 0.398$ ns, which are almost the same. This suggests that the slope does not affect the DCD and the SDR link calibration (systematic uncertainty) is stable and perfectly consistent with that of the SATRE link during the six months.

Figure 4.1.2 shows the TDev of the SDR and SATRE TWSTFT results illustrated in Figure 4.1.1. Here the SDR link stability given by the 6-month data set is more evident than for the monthly data set (cf. Figure 3.1.1). For averaging times within one day, the gain factor is between three and five. After three days however, the gain is diminished. This is considered reasonable as the diurnal effect is averaged out beyond three days.

4.2 Long-term consistency between SDR TWSTFT and GPS PPP links

Figure 4.2.1 illustrates the SDR link compared to the PPP link over 750 days for the baseline of TL-KRIS. The PPP data are extracted from *Circular T*. The $\sigma(\text{DCD}) = 0.92$ ns within the combined uncertainty of the SDR link and PPP in the DCD. This early study did not take into account the long-term variation (the slope) between TWSTFT and GPS.

Figure 4.2.2 shows the six months' SDR and PPP links and the DCD(SDR-PPP) over the baseline of OP-PTB. As can be seen, there is an obvious tendency in the DCD: a slope of 2.22 ns/year, as described in [9, 10], the so-called long-term variation between TWSTFT and GPS. In Section 4.1 we showed that the SDR link is consistent with the SATRE link, and there is roughly the same slope of 1.98 ns/year in the DCD(SATRE-PPP) as shown in Figure 4.2.3. The difference between 2.22 ns and 1.98 ns per year is negligible compared to the measurement noise and the diurnals in the SATRE link. Whereas the SDR-SATRE comparison can only show the combined effect of delay changes in the two SATRE and SDR receive parts, SDR-GPS and SATRE-GPS disclose all kinds of delay changes in both sets of equipment. Thus a larger slope was to be expected, and of course efforts are needed to identify the root cause and then reduce it closer to zero. We consider the observed slope as a systematic drift of either GPS time transfer or TWSTFT or both, independently of the use of SATRE or SDR receivers. In our further analysis we remove the linear trend and analyse the residual data to investigate other processes of instability in the SATRE and SDR links with respect to the PPP link.

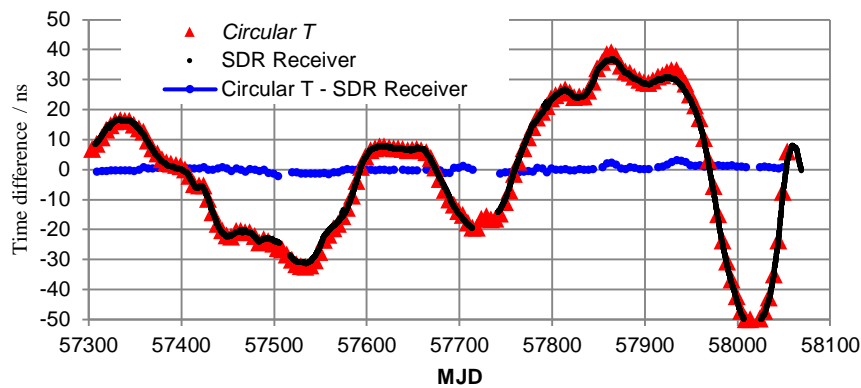


Figure 4.2.1. SDR link compared to PPP link during MJDs 57304-58054 with $\sigma(\text{DCD}) = 0.92$ ns. The PPP data are extracted from *Circular T*.

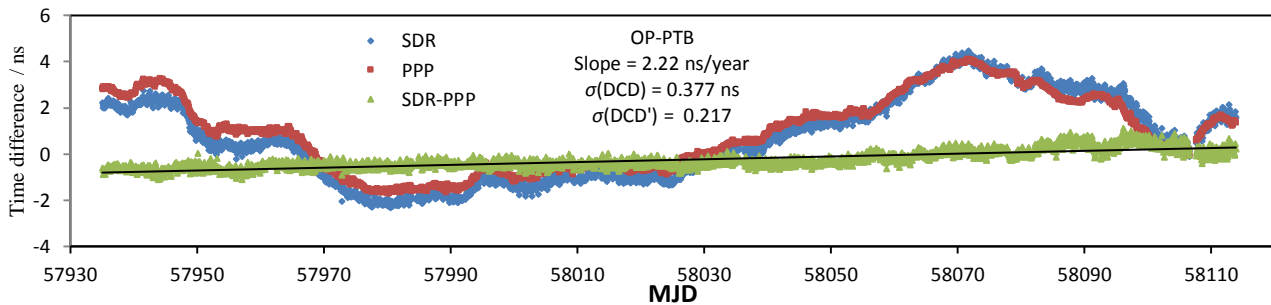


Figure 4.2.2 Six months' SDR and PPP links and the DCD(SDR-PPP) over the baseline of OP-PTB with a slope of 2.22 ns/year, $\sigma(\text{DCD}) = 0.377$ ns and with $\sigma(\text{DCD}') = 0.217$ ns.

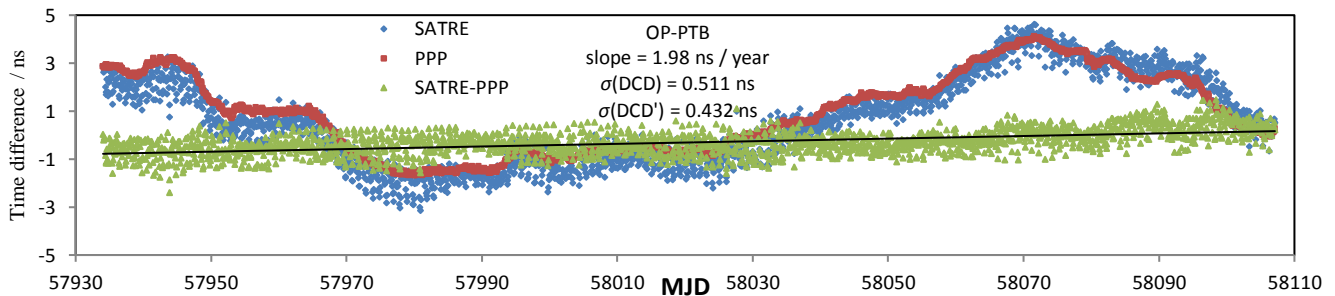


Figure 4.2.3 Six months' SATRE and PPP links and the DCD(SATRE-PPP) over the baseline of OP-PTB with a slope of 1.98 ns/year, $\sigma(\text{DCD}) = 0.511$ ns and with $\sigma(\text{DCD}') = 0.432$ ns.

When DCD' is used as the DCD after removing the slope, cf. Figures 4.2.2 and 4.2.3, the $\sigma(\text{DCD}) = 0.511$ ns and $\sigma(\text{DCD}') = 0.432$ ns for the SATRE-PPP comparison and $\sigma(\text{DCD}) = 0.377$ ns and $\sigma(\text{DCD}') = 0.217$ ns for the SDR-PPP comparison. Noting that the conventional statistical uncertainty for PPP is $u_A = 0.3$ ns and the standard deviation for the SDR-PPP comparison is $\sigma(\text{DCD}') = 0.217$ ns, the results show very good consistency between the SDR and PPP links. In other words, over the long-term, the SDR link is as statistically stable as that of SATRE and GPS. Table 4.2.1 gathers the statistical results of the DCD and the DCD'. Here the 'Slope affecting factor' indicates by how much the long-term systematic stability may affect the link comparisons.

Table 4.2.1 Agreement between SATRE, SDR and PPP links over the baseline of OP-PTB (comparing the DCD before/after removing the slope)

DCD (1)	Slope / ns/year (2)	$\sigma(\text{DCD})$ /ns (3)	$\sigma(\text{DCD}')$ /ns (4)	Slope affecting factor (3)/(4)
$\sigma(\text{SATRE-SDR})$	0.279	0.400	0.398	1.00
$\sigma(\text{SATRE-PPP})$	1.980	0.511	0.432	1.18
$\sigma(\text{SDR-PPP})$	2.220	0.377	0.217	1.73

By using the $\sigma(\text{DCD}')$, we can compute the gain factor of the SDR links. From $\sigma[\text{DCD}'(\text{SATRE-PPP})]$ and $\sigma[\text{DCD}'(\text{SDR-PPP})]$ in Table 4.2.1, the gain factor is $0.432/0.217 = 2.0$. The true factor values could be larger than 2.0 because it also contains the uncertainty of PPP that may be about 0.1 ns to 0.3 ns.

Table 4.2.2 Agreement between SDR and PPP links over different UTC baselines (comparing the DCD before/after removing the slope)

Baseline (1)	Slope / ns/year (2)	$\sigma(\text{DCD})$ /ns (3)	$\sigma(\text{DCD}')$ /ns (4)	Slope affecting factor (3)/(4)
OP-PTB	2.2	0.377	0.217	1.7
CH-PTB	2.7	0.374	0.222	1.7
IT-PTB	2.4	0.695	0.431	1.6
TL-KRIS	2.9	0.313	0.188	1.7
Mean		0.440	0.264	1.7

Finally, the long-term stability in the SDR links using the baselines in Europe and Asia was estimated. The results are given in Table 4.2.2. The mean value $\sigma(\text{DCD}') = 0.264$ ns is smaller than the conventional statistical uncertainty $u_A = 0.3$ ns of the PPP [1] showing a very good statistical stability agreement between the SDR and PPP links. The mean value of the slope affecting factor is 1.7. This suggests that roughly speaking, $\sigma(\text{DCD})/1.7$ is the real standard deviation (statistical instability) of the difference between the TWSTFT and GPS links.

From the 6-month data analysis, we observe that SDR TWSTFT is statistically stable relative to SATRE TWSTFT. However, SDR TWSTFT and GPS PPP links over some baselines exhibit a systematic deviation similar to the comparison of SATRE TWSTFT and GPS PPP links. After removing the linear deviation, SDR TWSTFT is stable and consistent with respect to GPS PPP results. It should be pointed out that when the 6-month data set is used to compute annual variations, the slopes given in this section may not be exact but can be used as a benchmark. Readers who are interested in the long-term variation between TWSTFT and GPS links may refer to [9, 10].

5. Summary

The SDR TWSTFT pilot study started about two years ago. In this paper, we reviewed the history, technical aspects and settings, as well as the major results of the pilot study. We also presented the results of the BIPM final evaluation that used the approaches of direct SDR and SATRE link comparisons, triangle closure comparisons and the comparison with GPS PPP or IPPP as reference. The evaluation used SATRE TWSTFT, SDR TWSTFT, GPS PPP, and GPS IPPP data to examine the performance of the SDR TWSTFT with the standard UTC generation procedure, Tsoft. Starting from October 2017 (*Circular T 359*), the SDR TWSTFT has been used as a backup UTC time link. The results are, and will continue to be, published monthly on the BIPM website, e.g. the link and link comparison results of November 2017 can be found in [16-18].

To summarize the work of the BIPM's final evaluation and the pilot study, we can conclude that:

- the monthly data analysis confirmed again that SDR TWSTFT improves the short-term (for averaging times up to three days) stability of SATRE TWSTFT by reducing the diurnal and the measurement noise for all the baselines;
- the six-month data analysis showed that SDR TWSTFT calibration is stable in the long-term when compared to SATRE TWSTFT;
- for some baselines, SDR TWSTFT showed a long-term deviation between SATRE TWSTFT and GPS PPP or GPS IPPP links, after removing the linear trend, SDR TWSTFT is statistically stable compared to GPS PPP or IPPP;
- the BIPM has validated the SDR TWSTFT results for the Asia-to-Asia, Asia-to-Europe, Europe-to-Europe and Europe-to-USA links using three different satellites operating in the Ku-band;
- most of the SDR TWSTFT participants have implemented the settings for facilitating the use of SDR TWSTFT data in UTC computation;
- the BIPM has made test runs using SDR TWSTFT data in UTC generation and has started using SDR TWSTFT as backup time links since October 2017;
- the use of SDR TWSTFT in UTC generation will be implemented in 2018, based on the link-by-link decisions made by the BIPM and the link participants;
- for the computation of *Circular T*, the uncertainty components of the SDR TWSTFT are by convention: u_A of 0.2 ns, u_B equal to the corresponding uncertainty of the SATRE link if the SDR link is not independently calibrated;
- further improvements of SDR TWSTFT is possible by fully using the redundancy in UTC time transfer networks [11];
- a significant work remains to be done with the SDR link calibration issue: a joint study by the BIPM and the WG on TWSTFT is ongoing;
- from a technical and practical point of view, the SDR TWSTFT is now ready to be accepted for UTC time links.

The SDR is an open platform for operators of TWSTFT ground stations. Laboratories may undertake further (or more in-depth) studies, including the use of the carrier phase information for various applications [13] or by developing a complete SDR transmission and reception platform as an alternative to the modem technique for two-way time and frequency transfer.

ACKNOWLEDGMENTS

The authors acknowledge Tadahiro GOTOH and Wen-Hung TSENG for their earlier contributions to this study. We thank Gérard PETIT and Julia LEUTE for supplying the IPPP data and Andreas BAUCH for helpful advice.

This paper includes contributions from the U.S. Government and is not subject to copyright.

REFERENCES

- [1] BIPM *Circular T 360*, January 2018, <ftp://ftp2.bipm.org/pub/tai/Circular-T/cirhtm/cirt.360.html>
- [2] TWSTFT Calibration Guidelines for UTC Time Links V2016 <ftp://tai.bipm.org/TFG/TWSTFT-Calibration/Guidelines>
- [3] HUANG Y J, TSENG W H, LIN S Y, YANG S H and FUJIEDA M (2016) TWSTFT Results by using Software-Defined Receiver Data, Proc. European Frequency and Time Forum 2016, York, UK, April 2016, pp. 137-140
- [4] HUANG Y J, FUJIEDA M, TAKIGUCHI H, TSENG W H, and TSAO H W, “Stability improvement of an operational two-way satellite time and frequency transfer system,” *Metrologia*, vol. 53, no. 2, pp. 881–890, Mar. 2016
- [5] Recommendation CCTF 5 (2017), On improving the Uncertainty of Two-Way Satellite Time and Frequency Transfer (TWSTFT) for UTC Generation, <http://www.bipm.org/en/committees/cc/cctf/publications-cc.html>
- [6] Recommendation ITU-R TF.1153-4 (08/2015), The operational use of two-way satellite time and frequency transfer employing pseudorandom noise codes (Geneva, Switzerland)
- [7] ZHANG V, ACHKAR J, HUANG Y J, JIANG Z, LIN S Y, PARKER T and PIESTER D (2017) A Study on Using SDR Receivers for the Europe-Europe and Transatlantic TWSTFT Links, Proc. 48th Annual Precise Time and Time Interval Systems and Applications Meeting, Monterey, California, USA, January 2017, pp. 206-218
- [8] JIANG Z, ARIAS F, ZHANG V, HUANG Y J, ACHKAR J, PIESTER D, LIN S Y, WU W, NAUMOV A, YANG S, NAWROCKI J, SESIA I, SCHLUNEGGER C, LIANG K and FUJIEDA M (2018) Implementation of SDR TWSTFT in UTC Computation, Proc. 49th Annual Precise Time and Time Interval Systems and Applications Meeting, Reston, Virginia, USA, January 2018, pp. 184-208
- [9] JIANG Z, MATSAKIS D and ZHANG V (2017) Long-term instability in UTC time links, Proc. 48th Annual Precise Time and Time Interval Systems and Applications Meeting, Monterey, California, January 2017, pp. 105-126
- [10] LIN S Y and JIANG Z (2018) The Long Term Stability and Redundancy Test of GPS Multi-Receiver Ensemble, Proc. 49th Annual Precise Time and Time Interval Systems and Applications Meeting, Reston, Virginia, USA, January 2018, pp. 154-163
- [11] JIANG Z, ZHANG V, PARKER T E and PETIT G (2018) Reducing the diurnal affections in TWSTFT for UTC Time Transfer using Redundant Links using redundant links, submitted to *Metrologia*
- [12] PETIT G, KANJ A, LOYER S, DELPORTE J, MERCIER F and PEROSANZ F (2015), 1×10^{-16} frequency transfer by GPS PPP with integer ambiguity resolution, *Metrologia*, vol. 52 (2015) 301–309
- [13] FUJIEDA M, PIESTER D, GOTOH T, BECKER J, AIDA M and BAUCH A (2014), Carrier-phase two-way satellite frequency transfer over a very long baseline, *Metrologia*, vol. 51 (2014) 253-262
- [14] PIESTER D, BAUCH A, BECKER J, STALIUNIENE E, SCHLUNEGGER C (2008) On Measurement Noise in the European TWSTFT Network, IEEE Trans. UFFC, vol. 55, no. 9, pp. 1906-1912
- [15] PIESTER D, BAUCH A, BREAKIRON L, MATSAKIS D, BLANZANO B, KOUDELKA O (2008) Time Transfer with nanosecond accuracy for the realization of International Atomic Time, *Metrologia*, vol. 45, no. 2, pp. 185-198
- [16] <ftp://ftp2.bipm.org/pub/tai/timelinks/lkc/1711/opptb/lnk/opptb.ttts.gif> for the SDR link
- [17] <ftp://ftp2.bipm.org/pub/tai/timelinks/lkc/1711/opptb/dlk/opptb.tts5.gif> for the comparison of SDR and SATRE links
- [18] <ftp://ftp2.bipm.org/pub/tai/timelinks/lkc/1711/opptb/dlk/opptb.t3sa5.gif> for the comparison of SDR and GPSPPP links